Synthesis and optimization of stapled DOCK peptides with improved drug-like properties

Atiruj Theppawong,* Ewout De Geyter, and Annemieke Madder*

Department of Organic and Macromolecular Chemistry, Ghent University, Krijgslaan 281 S4, 9000 Ghent, Belgium
Email: Atiruj.theppawong@ugent.be and Annemieke.Madder@UGent.be

This article is dedicated to our distinguished colleague and friend Professor Léon Ghosez

Abstract

Protein-protein interactions (PPIs) involving short α-helix fragments are of critical importance in cellular processes. Stapling of α-helical peptides improves their conformational stability, affinity, and resistance to proteases. ELMO proteins (ELMO1 and ELMO2) play a crucial role in cellular processes, and recent studies highlight ELMO1's distinct role in interacting with, and modulating, DOCK2 levels. To harness the full therapeutic potential of peptides mimicking the DOCK protein for interference with the ELMO/DOCK interaction, we propose employing deoxycholic acid and conventional small molecules for stapling, thus enhancing the therapeutic potential of these peptides. Our method employs solid-phase peptide synthesis, strategically incorporating two cysteine amino acids to create well-defined, constrained cyclic peptides upon stapling. In addition to their structural stabilisation, these stapled peptides exhibit remarkable proteolytic stability, defying enzymatic degradation, even in the presence of human serum.
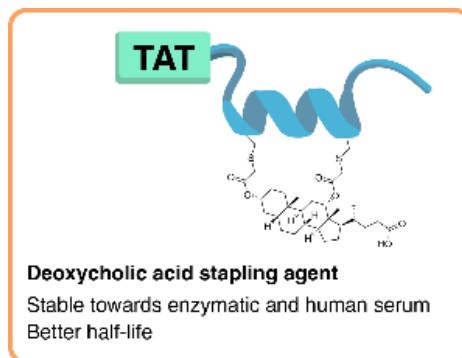
TAT

Deoxycholic acid stapling agent
Stable towards enzymatic and human serum
Better half-life

Introduction

Proteins play a pivotal role in many aspects of cellular systems. Their roles range from structural stabilization and the transport of nutrients, ions and small molecules over complex biological processes, to enzymatic reactions.[1] Protein-protein interactions (PPIs) are defined as specific physical interactions between protein pairs that occur by selective molecular docking in a particular biological context.[1] These associations originate from, and owe their specificity to, supramolecular forces such as electrostatic interactions, hydrogen bonding and hydrophobic effects.[1,2] Simplifying interacting proteins into structural elements, and locking their functional conformation via synthetic manipulation, is a promising approach to bridge the targeting space gap between small molecules and biologics.

It is well documented that over fifty percent of PPIs involve short α-helical fragments from the involved proteins.[3,4] Short peptides are generally unstructured in aqueous solution as water molecules compete with the intramolecular hydrogen bonding of the peptide backbone. This denatured conformation in solution is also entropically favorable. As a result, short, isolated peptide fragments usually lose their affinity for the target as a consequence of this structural instability. Conformational rigidification of α-helical peptides has been shown to reduce the entropic penalty for target binding, which potentially allows increasing target affinity.[5] Indeed, short peptides can be induced to fold into protein-like bioactive conformations (strands, helices, turns) by proper cyclization through various so-called stapling methodologies.[6] This can be achieved by using various non-peptide molecular constraints (stapling molecules) that help to fine-tune three-dimensional (3D) structures.[7] Interestingly, by hiding the amide bonds inside the helix, this conformation is also more resistant to proteases,[8] and has further been demonstrated to more easily permeate into the cellular membrane.[9,10] These two characteristics are critical for an efficient therapeutic use of such peptides, especially for intracellular targets.

The engulfment and cell motility protein 1 (ELMO1) is a scaffolding component of the Elmo-Dock complex. It interacts with DOCK (dedicator of cytokinesis)180, a large protein (~180 kD) involved in a variety of cellular functions, which is essential for activation of Rac GTPase-dependent biological processes. Its C-terminal pleckstrin homology (PH) domain mediates direct interaction with DOCK180, and is critical in Rac signaling, a process implicated in the control of cell-cell adhesions, cell-matrix adhesions, cell migration, cell-cycle progression and cellular transformation.[11] ELMO1 also interacts with DOCK2 and plays a role in controlling DOCK2 levels and DOCK2-dependent T-cell migration in primary lymphocytes.[12,13] ELMO1 has been linked to invasive phenotypes of cancer cells.[14–16]
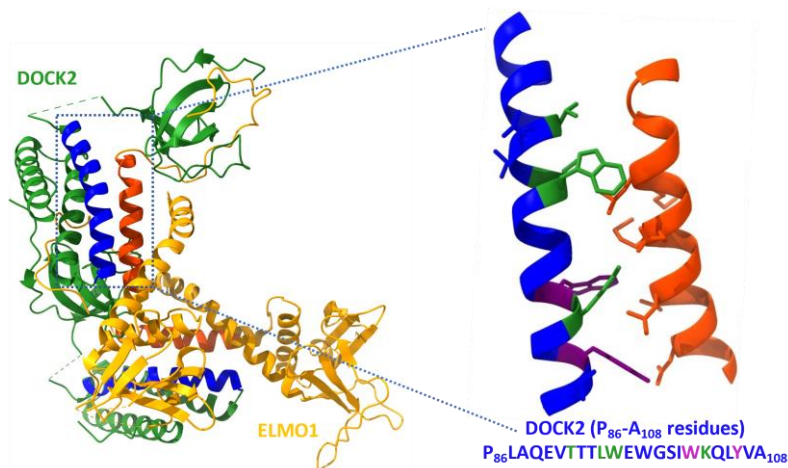

Scheme 1. ELMO1:DOCK2 complex from PDB code 3a98[17] (left) with detail of DOCK2 amino acids (86–108 region) in blue and ELMO1 target helix in red (right). The structure was visualized using ChimeraX-1.7 software.

More recently, the Ravichandran group identified multiple single-nucleotide polymorphisms (SNPs) in ELMO1 and DOCK2 genes, associated with the outcome of rheumatoid arthritis.[18] The same group reported the involvement of ELMO1 signaling in osteoporosis, with a decrease in bone resorption in wild-type osteoclasts (*in vitro*) induced by treatment with an ELMO1 binding peptide. This peptide, designed from a DOCK2 α-helix interacting with ELMO1 and associated with a Tat sequence, is suggested to impair the ELMO/DOCK interaction, inhibiting the ELMO1 signaling pathway. While promising, the use of such a peptide as a therapeutic agent is well known to face limited in-vivo stability, as well as a random conformational structure, that would hamper its binding to the specific target. To address these limitations, we propose to apply a versatile stapling methodology to the 23-mer ELMO1-interacting peptide, using an amphipathic molecule (deoxycholic acid) on the one hand, and conventional small molecules (e.g., 4,4'-Bis(bromomethyl)biphenyl for *i,i+7* and 1,3-Bis(bromomethyl)benzene for *i,i+4*) on the other hand. In this work, we used solid-phase peptide synthesis (SPPS) for preparing a diversity of linear peptides incorporating two cysteine amino acids (Cys) in different positions (*i,i+7* and *i,i+4*). The thiol group (-SH) of the cysteines is prone to engage in S_N2 nucleophilic substitution, and by reaction with bifunctional templates, constrained cyclic peptides can be generated.

Results and Discussion

Peptide synthesis and optimization

In previous work, a DOCK (wt)-mimicking peptide consisting of 23 amino acids was designed based on critical ELMO1-interacting residues of DOCK2.[19] As discussed above, stapled peptides are an emerging class of cyclic-peptide molecules with enhanced biophysical properties such as conformational and proteolytic stability, improved cellular uptake, elevated binding affinity, and specificity for their biological targets.[20–24] Among the limited number of chemistries available for their synthesis, the cysteine-based stapling strategy[25–27] has received considerable attention in the last few years, driven by facile access to cysteine-functionalized peptide precursors. To accomplish this, the cysteine pair must be included at positions that facilitate the macrocyclization of the peptide and, ideally, do not compromise target binding. For instance, in an α-helical peptide, residues located at the (*i,i+4*) or (*i,i+7*) positions reside on the same face of the helix and are, therefore, strategic points to place two cysteines in the sequence.[7] In this work, we aimed to synthesize DOCK peptide variants containing two cysteines; in one series, the cysteine (Cys, C) residues are located in positions *i* and *i+4* and, in a second series of analogues, they are located in positions *i* and *i+7*. Subsequently, both peptides will be stapled using three different crosslinkers (see scheme 2). Moreover, to allow and boost delivery of DOCK peptides across the plasma membrane or endosomal uptake[28], we fused it to the TAT-sequence, to generate cell-penetrating peptides (TAT-DOCK), which can offer potential for therapeutic intervention.[29,30]
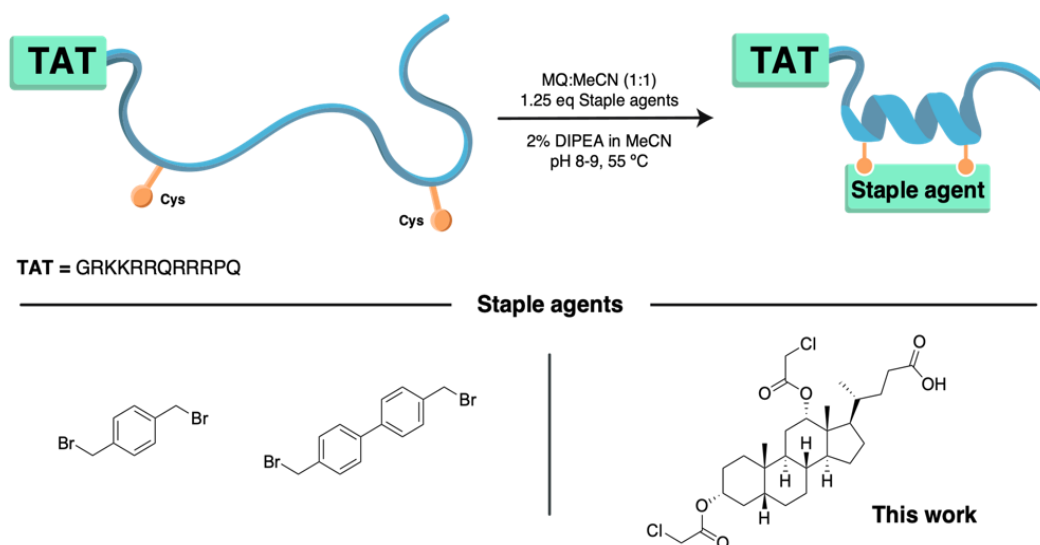
Scheme 2. General stapling methodology for TATDOCK (*i,i+7* and *i,i+4*) peptides and scrambled versions thereof

Wild-type TAT-DOCK (TDWT), *i,i+7*-stapled TAT-DOCK (TD, *i,i+7*) and *i,i+4*-stapled TAT-DOCK (TD, *i,i+4*) peptides were synthesised along with their scrambled variants, wild-type TAT-DOCK scrambled (TSWT) and stapled TAT-DOCK scrambled versions, using various coupling procedures on PEG-based resins, introducing amide functions at both the N- and C-termini (Table 1). It is well known that coupling reagents play crucial roles in the iterative construction of amide bonds for the synthesis of peptides and peptide-based derivatives. First, the classical HBTU/DIPEA combination was used on two different resins, including Fmoc-Rink Amide AM resin (0.69 mmol/g) and ChemMatrix® Resin (0.5 mmol/g) for TATDOCK (*i,i+7*), in order to compare the yield and purity of the syntheses of these rather long peptides (see supporting information in Supplementary Material). In the first case, the target peptide was obtained with quite low yields, however, ChemMatrix® resin gave slightly better yields (Table 1). Therefore, further optimization of coupling cocktails was performed on the low-loading PEG-resins ChemMatrix® and NovaPEG® Rink amide LL resin. It has been reported that the coupling reagent Oxyma displays a remarkable capacity to inhibit racemization. It features impressive coupling efficiency in both automated and manual syntheses, superior to that of HOBt and at least comparable to that of HOAt, surpassing the latter coupling agent in the more demanding peptide models.[31] Therefore, Oxyma/DIC has gained a lot of attention for peptide synthesis due to its rapid, robust, and safe properties as a coupling mixture.[31,32] When comparing final isolated yields, ChemMatrix® resin allowed us to obtain more target peptide when compared to NovaPEG® Rink amide resin. However, since the isolated yield remained low, we continued trying to maximize the yield and purity of these long TATDOCK peptides.

Several studies have shown that the addition of bases to coupling reagents can improve the yield during the assembly of such complex or long peptides.[33] We, therefore, also investigated the effect of an Oxyma/DIC: DIPEA (1:0.05M ratio) coupling combination.[34,35] N,N-Diisopropylethylamine (DIPEA) (also known as Hünig's base) is an aliphatic amine with a pKaH of 10, and provides good activation for the class of phosphonium- or uronium-based coupling reagents.[34] This approach was applied to the difficult TATDOCK peptide synthesis and resulted in a considerable improvement in isolated yield when compared to Oxyma/DIC without a base. Moreover, Albericio's research group observed that EDC·HCl/K-Oxyma gave short peptides (5 mers) with double the purity obtained with Oxyma/DIC.[36] Therefore, in a final attempt for optimisation, we decided to replace DIC with EDC, but still have a base, DIPEA, as an additive agent. Carbodiimides such as DIC and EDC have been demonstrated

to reduce the level of racemization, and enhance the coupling yields as they reduce the reactivity of the active species formed in the reaction, thus, inhibiting side-reactions such as the formation of *N*-acylureas and oxazolones.[37] Under these final optimized conditions, the isolated peptide was obtained in good purity with an isolated yield of 32%, which represents a five-fold improvement in comparison with the first conditions tried (Table 1). Afterwards, the optimized methodology was applied to the synthesis of TATDOCK (*i,i+4*) and the outcome was in line with that for TATDOCK (*i,i+7*).

Notably, the final deprotection also influenced the isolated yield of TATDOCK peptides due to the cation-alkylation of an amino-acid side chain (e.g., Trp, W). We obtained a +56 mass of the crude peptide, which could relate to *t*-Bu cation attack on the peptide backbone. To minimise formation of side products, the deprotection was necessarily conducted in a very diluted environment (ca. 1-2 mg resin per 1 mL cocktail solution), and in an optimised cocktail solution recipe (see experimental section).

Table 1. Yield improvement of TATDOCK(s) peptides via various coupling procedures on different PEG-based resins

Peptide	Sequences			
TD (*i,i+7*)	GRKKRRQRRRPQPLAQEVTTTLWECGSIWKQCYVA-NH$_2$			
TS (*i,i+7*)	GRKKRRQRRRPQEGWASYWLKLAQCPTTQIVCVET-NH$_2$			
TDWT	GRKKRRQRRRPQPLAQEVTTTLWEWGSIWKQLYVA-NH$_2$			
TSWT	GRKKRRQRRRPQEGWASYWLKLAQWPTTQIVLVET-NH$_2$			
TD (*i,i+4*)	GRKKRRQRRRPQPLAQEVTTTLWCWGSCWKQLYVA-NH$_2$			
	% Isolated Yield			
Peptide	**HBTU/DIPEA**	**Oxyma/DIC**	**Oxyma/DIC: DIPEA**	**Oxyma/EDC: DIPEA**
TD (*i,i+7*)	4.8^{Rink}, 6.0^{chem}	5.1^{Nova}, 10.1^{chem}	16.2	32
TS (*i,i+7*)	ND	ND	7.0*	ND
TDWT	ND	4.2	10.0	ND
TSWT	ND	ND	12.0	ND
TD (*i,i+4*)	ND	9.8	14.0	33

Synthesis scale (25-50 μmol), Rink: Fmoc-Rink Amide AM resin (0.69 mmol/g), Chem: ChemMatrix® Resin (0.5 mmol/g), Nova: NovaPEG® Rink amide LL resin (0.17 mmol/g), DIC:DIPEA or EDC:DIPEA (1:0.01, ratio), * indicates considerable amounts of a side-product with +56 mass (*t*-bu cation). ND = not determined.

Peptide stapling methodology

The synthesized *i,i+4* and *i,i+7* peptides were stapled using the commercially available crosslinkers α,α'-dibromo-*m*-xylene[38,39] and 4,4'-bis(bromomethyl)biphenyl[20,21,24] as well as a specifically generated deoxycholic acid (DCA) derivative. DCA is a bile acid, which are steroid derivatives from cholesterol found in the bile fluid. These steroid molecules consist of a rigid scaffold and can be used to provide conformational restriction to the attached peptide. We have earlier been able to demonstrate that peptides stapled with such a deoxycholic acid moiety show increased uptake in RAW264.7 mouse macrophages.[40] A suitable DCA derivative for stapling can be obtained (Scheme 3) from the reaction of the parent bile acid with α-chloroacetylchloride.
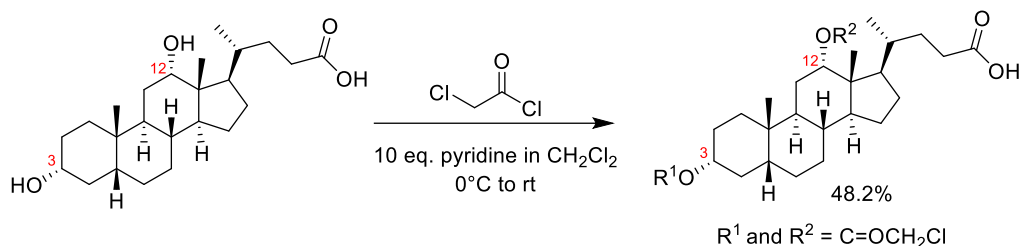
Scheme 3. Deoxycholic acid derivative synthesis

After completion of the peptide synthesis and cleavage from the solid support, the stapling reaction was carried out under *in-house* optimized conditions (Scheme 2), involving a mixture of water and acetonitrile (MeCN) at pH 8-9, and carried out at a concentration of around 0.5-1.0 mg/mL. The desired stapled peptides were obtained in a range of moderate-to-excellent yields (38-97%, Table S2 Supplementary Material). For the DCA-stapled peptides, the two regioisomeric stapled products were not separated; the mixture was used as such for further analysis and testing.

Circular Dichroism (CD) Spectroscopy

In order to verify whether the synthesized stapled peptides were able to adopt a helical conformation, CD spectroscopy was carried out. CD experiments were supportive of the helical character of TATDOCK peptides, but only for the stapled peptides, and only in the presence of 10% and 50% trifluoroethanol. Trifluoroethanol (TFE) has been used for many decades to denature proteins and stabilize structures in peptides.[41,42] The linear peptides and the stapled peptides showed either random coil conformations or minimal helix tendencies in the miliQ water used. The effect of TFE on peptide folding and unfolding was also studied (see Supplementary Material, CD section). In fact, in dilute aqueous solution, TFE increases helicity (see supporting data in Supplementary Material) by selectively destabilizing amide functions that are solvent exposed, with the consequence that compact conformations are monitored.[41] Moreover, the ratios of ellipticities at θ_{222} and θ_{208} were calculated (see supporting data). The $\theta_{222}/\theta_{208}$ ratios provide information on the likelihood of the α-helix being in isolation or found within a coiled-coil structure.[43–46] A ratio of approximately 0.9 or less indicates the former, whereas a ratio above 1.0 typically indicates the latter.

The effect of adding 50% trifluoroethanol, a strong helix-promoting solvent additive,[41] to a solution of the TATDOCK peptides is shown in Figure 1. As expected, spectra typical of α-helical peptides can be observed. Comparing the original TATDOCK (*i,i+4*) and TATDOCK (*i,i+7*) series with the scrambled TATDOCK series revealed significant differences in terms of helicity and θ_{222} (see Supplementary Material supporting information in Table S4). It is clear that the scrambled sequences do not display α-helical character even when fused with the stapling agents (DCA, BP and X, Figure S16). The CD spectra of the *i,i+7* sequences are shown in Figure 1A, indicating the potential of the stapled sequences to adopt helical conformations with slight differences depending on the specific staple. The CD spectra of the *i,i+4* sequences are shown in Figure 1B. TATDOCK (*i,i+4*) peptides showed comparable % helicity and θ_{222} for DCA and X staple analogues, but the BP-stapled analogue seems to have lost the capacity to adopt a helical conformation. The BP-stapling agent is commonly used in *i,i+7* stapling for retaining the helical structure.[20,21,24] This could mainly explain why TATDOCK (*i,i+4*) BP showed less helix conformation based on CD results. Remarkably, the DCA moiety offered more flexibility when combined with *i,i+4* sequence, which shows the advantage of utilizing this stapling methodology.

A   **B**
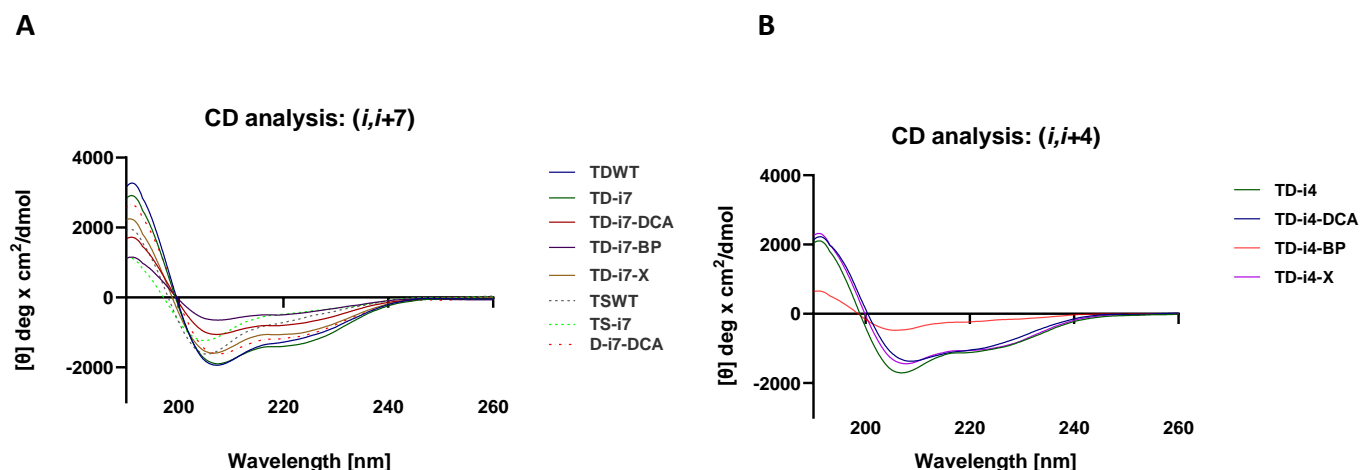
Figure 1. CD spectra of A: the stapled TATDOCK (*i,i+7*) and linear TATDOCK peptides (*i,i+7*), left; B: the stapled TATDOCK (*i,i+4*) and linear TATDOCK peptides (*i,i+4*), right. The peptides were dissolved in 1:1 TFE/H$_2$O at a final concentration of 20 µM.

Peptide stability

Proteolytic stability against α-Chymotrypsin

For the obtained stapled peptides, stability against proteolytic degradation was assessed. Indeed, protease stability is a key consideration in the development of peptide-based drugs. All organisms contain proteases, which have an important influence on: (1) physiological processes, such as digestion, hemostasis, cell death programming/apoptosis , signal transduction, reproduction and the immune response, and (2) disease states such as cancer, viral infection, Alzheimer's disease, inflammatory and cardiovascular disorders.[47] α-Chymotrypsin (a serine endopeptidase) preferably cleaves peptide bonds at the C-terminal side of large hydrophobic residues, such as phenylalanine (Phe, P), tyrosine (Tyr, Y), tryptophan (Trp, W) and leucine (Leu, L).[48–50] It was used here to obtain an idea about the potential of the different staples to protect the parent peptides from proteolytic degradation.
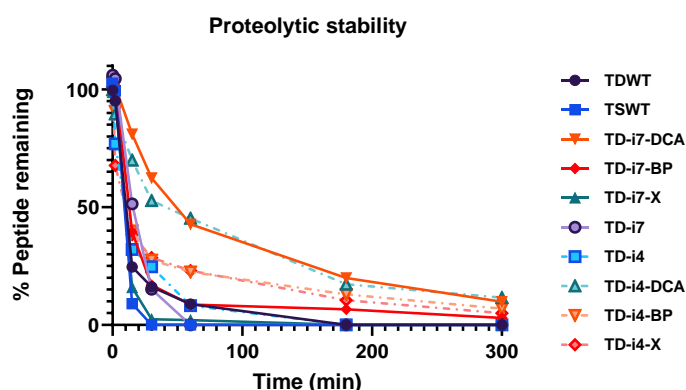

Figure 2. Digestion stability of the TATDOCK *i,i+7* and *i,i+4* series of peptides against 0.25 µg/mL of α-chymotrypsin. TD-i7 and TD-i4 refer to TATDOCK TD (*i,i+7*) and TD (*i,i+4*) sequences containing cysteine substitutions. The suffix DCA refers to peptides stapled with deoxycholic acid, BP to stapling with a bis-bromomethyl-biphenyl derivative and X to stapling with bis-bromomethylbenzene (cfr scheme 2), respectively. See experimental section for further details.

Unstapled TATDOCK substrates (TDWT, TSWT, TD-i7, TD-i4 in Figure 2) were used as controls to allow the comparison of the degradation profiles of unstapled versus stapled peptides. The stability of the peptides towards proteolysis by α-chymotrypsin was determined using analytical RP-HPLC. Each peptide was incubated with α-chymotrypsin; the starting peptides were quantified and characterized by means of integration of the area under the curve (AUC) at 214 nm over time. The results showed that all stapled peptides had gained significantly enhanced proteolytic stability towards α-chymotrypsin and that the DCA staple seems to confer the best protection from proteolytic degradation (Figure 2).

Human serum stability

The short half-life of peptides in human serum has been one of the major concerns of peptide drugs. Peptides are typically eliminated from the bloodstream within minutes to hours after IV administration. Consequently, the exposure to the target tissue may not be sufficient in order to have an *in vivo* effect. The determination of peptide stability in human serum constitutes a powerful screening assay for clearing unstable (i.e., fast-degradation) peptides from further peptide therapeutic development. Peptide stability in serum can be determined by RP-HPLC. Given the more labor-intensive nature of the serum stability test, and the enhanced performance of the *i,i+7* peptides in terms of helicity, we decided to focus on determining the serum stabilities of TATDOCK (wt), linear TATDOCK (*i,i+7*) and stapled TATDOCK (*i,i+7*). Three different serum concentrations (25%, 12.5%, and 6.25%, respectively) were explored in an effort to define conditions that allow clearly assessing the stability differences among the various sequences. To investigate the effects of the modifications on proteolytic susceptibility, the disappearance of the intact peptides incubated in diluted human serum (1X PBS buffer, pH 7.4) at 37°C was followed by RP-HPLC for up to 24 hours. Unstapled TATDOCK peptides showed fast degradation, and the combined effect of precipitation and aggregation could also be observed. Interestingly, the three stapled *i,i+7* peptides equipped with deoxycholic acid scaffold (DCA), biphenyl (BP) and phenyl (X) staples showed considerably increased stability in three different serum concentrations, which would be sufficient for further *in vivo* experiments. It could be noted that, at T_0, the unstapled peptides had been consumed by at least 50%. These experiments were conducted in the same way as the previous ones for both unstapled and stapled *i,i+7* series, however, extra methanol was added to prevent the precipitation of the peptides over time.
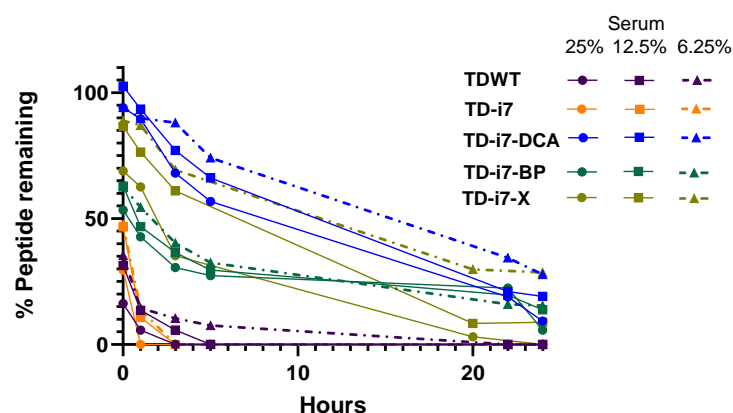
Figure 3. Human serum-stability profiles of unstapled wild type (TDWT) and cysteine substituted (TD-i7) TATDOCK peptides, and the *i,i+7* stapled TATDOCK series of peptides (with the suffix DCA referring to peptides stapled with deoxycholic acid, BP to stapling with a bis-bromomethyl-biphenyl derivative and X to stapling with bis-bromomethylbenzene respectively) in various concentrations of serum 25.0% (circle), 12.5% (rectangular) and 6.25% (triangle) in 1X PBS buffer, pH 7.4.

Conclusions

TATDOCK-stapled peptides were prepared using *i,i+4* and *i,i+7* stapling for enhanced intracellular interaction between ELMO and DOCK proteins. Next to more classical staples such as those derived from bis-bromomethylbenzene and a biphenyl analogue thereof, a deoxycholic acid analogue was developed to be compatible with a conventional cysteine-based stapling approach. Through systematic optimisation of various coupling protocols, we successfully established an optimal protocol for synthesizing the long TATDOCK peptides using either Oxyma/DIC:DIPEA or Oxyma/EDC:DIPEA. In terms of proteolytic stability, the stapled peptides (BP and DCA) in the *i,i+4* and *i,i+7* series showed more resistance towards α-chymotrypsin, proving that the stapled peptides provided extra benefits for further application. For human serum experiments, *i,i+7* series were selected to further examine their stability profile using various percentages of human serum. Whereas unstapled peptides showed fast degradation, stapled peptides showed more stable profiles. Interestingly, peptides conjugated using the DCA moiety exhibited the best drug-like property profile.

    As this field matures and stapling techniques become more well-documented, we expect to see more studies taking advantage of the combination of deoxycholic acid properties in the near future. The stapling approach presented will contribute to maximizing the chances of establishing effective peptide-based therapeutics for a variety of PPI targets. In view of earlier reports on the increased cell penetration capacities of DCA-modified sequences, DCA-stapled helical peptides might offer promising properties for targeting intracellular PPIs, which we will report on in due course.

Experimental Section

General. All-natural Fmoc-L-amino acids, coupling reagents 2-(1*H*-benzotriazol-1-yl)-1,1,3,3-tetramethyluronium hexafluorophosphate (HBTU), OxymaPure, N,N'-diisopropylcarbodiimide (DIC) and trifluoroacetic acid (TFA) were purchased from Iris Biotech GmbH. All peptides were synthesized using PEG-based resins, either the ChemMatrix® Rink Amide resin with a loading of ca. 0.5 mmol/g (0.4-0.6 mmol/g, Sigma Aldrich), Fmoc-Rink-amide AM resin (0.69 mmol/g, Iris Biotech) or NovaPEG® Rink amide resin LL (0.17 mmol/g, Sigma Aldrich). Peptide synthesis grade dimethylformamide (DMF) was purchased from Biosolve. Dichloromethane (DCM, HPLC grade), diethyl ether (Et$_2$O, HPLC grade), methanol (MeOH, HPLC grade), N,N-diisopropylethylamine (DIPEA), 1-ethyl-3-(3-dimethylaminopropyl)carbodiimide (EDC), N-methylmorpholine (NMM), tri-isopropylsilane (TIS), phenol, and acetic anhydride (Ac$_2$O) were obtained from Sigma Aldrich. 1,2-Ethanedithiol (EDT) was purchased from Janssen Chemica. α-Chymotrypsin type II and human serum AB plasma were acquired from Sigma Aldrich.

Deoxycholic acid derivative synthesis. An amount of 1000 mg of deoxycholic acid was dissolved in CH$_2$Cl$_2$ (15 mL) followed by addition of 10 eq. of pyridine (1.3 mL) into the solution and cooled in an ice bath at 0°C. Then, chloroacetyl choride (1.5 eq.) was added dropwise while stirring the solution. After 60 min, the reaction was stirred and gradually allowed to warm to room temperature and, subsequently, 0.5 eq of chloroacetyl chloride was added into the solution. Additionally, 0.5 eq and 0.25 eq. of chloroacetyl chloride were added into the solution after 120 and 180 min, respectively. After 260 min, the reaction was confirmed as showing no more C3 product. Finally, 10% HCl (1 volume) solution was then added to quench the reaction followed by extraction with dichloromethane (CH$_2$Cl$_2$, 3 X 20 mL). Combined organic layers were subsequently washed with water (2 X 20 mL) and brine (sat. NaCl, 2 X 20 mL) followed by drying over magnesium sulfate. The next step involved

evaporation of the organic solution and purification by means of column chromatography either using normal silica (using CHCl$_3$/EtOAc/TFA (89.9:10:0.1)) or preparative HPLC C18 silica (see supporting information in Supplementary Material), obtaining a white solid 48% (667 mg). **^{1}H-NMR** (300 MHz, CDCl$_3$): δ 5.18-5.11 (m, 1H), 4.80-4.66 (m, 1H), 4.04 (s, 2H), 4.00 (s, 2H), 2.42-2.11 (m, 2H), 1.93-0.94 (m, 24H), 0.88 (s, 3H), 0.79 (d, 3H, J= 4.8) , 0.71 (s, 3H). **LCMS** (ESI-MS, negative mode): found [M + ^{35}Cl]$^-$, *m/z* 580.10 and [M + ^{37}Cl]$^-$, *m/z* 582.09.

Peptide synthesis and optimization. All linear peptides were synthesized on a MultiPep RSi (Intavis) automated peptide synthesiser using the Fmoc-based strategy. In general, the synthesis of TATDOCK peptides was performed using 25-50 μmol scale resin of the PEGs based resins (Fmoc-Rink Amide AM resin (0.69 mmol/g), ChemMatrix® Resin (0.5 mmol/g), or NovaPEG® Rink amide resin LL (0.17 mmol/g)). For HBTU/DIPEA approach, synthesis with double coupling steps was performed as following: the resin was swollen in DMF for 30-60 minutes. A mixture of 5 equiv. amino acid in DMF (0.5 M), 5 equiv. HBTU in DMF (0.5 M) and 5 equiv. DIPEA in NMP (2 M) were added to the resin, with subsequent carried out for 40 minutes at room temperature per cycle. Afterwards, the reaction mixture was removed, and the resin was vigorously washed with DMF (6 x 60 sec). Every coupling was repeated for a second time. Fmoc group was usually removed using 40% piperidine in DMF (2 cycles for 4 min and 12 min, respectively) before adding a new solution of activated amino acid in order to connect a new monomer on the resin (elongation step) at the N-terminus. After each double coupling reaction was done, the capping step was then taken place (5 min) to cap all unreacted residues (free-NH) in order to prevent the deletion product formation followed the Fmoc-deprotection. The capping solution was prepared by mixing 5% of acetic anhydride and 5% of 4-methylmorpholine (NMM) in DMF. Before adding a new coupling reagent mixture (pre-activation for 5 min), the resin was washed with DMF (4 x 60 sec).

For the Oxyma/DIC approach, 1-10 mer peptides were produced with a single coupling for each residue. Afterwards, starting from 11-to-end mers, synthesis with double coupling steps was performed similar to HBTU/DIPEA. The resin was swollen in DMF for 30-60 minutes. A mixture of 5 equiv. amino acid in DMF (0.5 M), 5 equiv. Oxyma in DMF (0.5 M) and 5 equiv. DIC in NMP (1 M), 1:1:1 ratio, was poured into the resin to proceed the coupling reaction (30 min per cycle) at room temperature. The Fmoc moiety was usually removed using 20% piperidine in DMF (2 cycles for 7 min) before adding a new solution of activated amino acid in order to connect a new monomer on the resin (elongation step) at the N-terminus. The capping step for this procedure was not necessary in the peptide sequence protocol, but it is optional. The rest of the procedure was similar to the classical HBTU/DIPEA coupling approach.

For Oxyma/DIC:DIPEA and Oxyma/EDC:DIPEA, the synthesis was adopted from an optimised Oxyma/DIC methodology except for the addition of an extra 0.01 equiv. DIPEA into 1 M DIC solution as an accelerator in peptide coupling.

The coupling procedure (HBTU/DIPEA, Oxyma/DIC, Oxyma/DIC:DIPEA or Oxyma/EDC:DIPEA) was repeatably performed until the last monomer was included. Finally, Fmoc-deprotection was performed followed by a manual washing step of the resin with DMF (3X), MeOH (3X), DCM (3X) and Et$_2$O (3X). The completion of the deprotection reaction was analysed by the trinitrobenzenesulfonic acid (TNBS) test. A few beads were taken into a small Eppendorf tube, followed by treatment with 10 μL of 10% DIPEA/DMF and 10 μL of TNBS (1:1 ratio) at room temperature. Free amines were physically detected by a red colour change on the resins; otherwise, Fmoc-deprotection should be performed as an extra step before proceeding with the next step.

Small test cleavages of the TATDOCK peptides were performed during 60 min at room temperature using the following standard cleavage cocktail: 95% TFA, 2.5% TIS, and 2.5% H$_2$O. Afterwards, the resin was removed by filtration, and the majority of the cleavage cocktail was removed by nitrogen evaporation, followed by peptide precipitation using excess cold methyl tert-butyl ether (MTBE) and centrifugation at 10,000 rpm for 5 min. The

precipitated peptide was then re-dissolved in MQ:MeCN (1:1) and analysed by MALDI-TOF-MS. Once the results were satisfactory, we proceeded with the large scale deprotection with an optimised cocktail solution (TFA:EDT:TIS:H_2O:Phenol:1mg/mL Trp -> 91.5:2.5:2.5:2:1:0.5) in order to minimise the cation conjugation on the final product. The reaction was conducted for 2 hours in diluted conditions (1-2 mg resin/ mL of cocktail solution), followed by an evaporation step and peptide precipitation. For the large-scale cleavage, centrifugation (8 min, 8000 rpm at 4°C) was carried out. The supernatant was discarded and a fresh volume of cold MTBE was added to repeat the sonication and centrifugation in order to get rid of all scavengers. The crude peptide was subjected to purification by reverse phase HPLC depending on the scale of product (*vide infra* peptide purification section). All obtained peptides appeared as amorphous white solids.

Peptide stapling. Linear peptides (containing 2 cysteines) were dissolved in a mixture of MeCN and milliQ water (1:1 ratio) in order to obtain a 1.0 mg/mL concentration at room temperature. The reducing agent (tris(2-carboxyethyl)phosphine, TCEP) was then prepared at 10 mg/mL stock in milliQ water, and also the stapling reagent (deoxycholic acid derivative, *m*-xylene or 4,4'-Bis(bromomethyl)biphenyl) in MeCN at 2-5 mg/mL, depending on the maximum solubility of each stapling molecule. Afterwards, 1.0 eq. of TCEP was added to the peptide solution and allowed to vigorously stir for at least 20 min at room temperature. Then, the pH of the peptide solution was slowly adjusted to pH 8-9 using 2% DIPEA in MeCN (ca. 100-200 μL) followed by slightly increasing the temperature to 55 °C. At pH 8-9, the stapling reagent (1.25 eq.) was added to the mixture and homogeneously stirred for up to 1-2 hours. After a while, the reaction turned turbid. The conversion of starting peptide was analysed through analytical HPLC (Agilent 1260 infinity II, equipped with Chromolith® High resolution, RP-18e, 50-4.6 mm, 0-100% for 7 min at 35°C) by monitoring the appearance of the expected product peak, and also the shift in t_R. When sampling the solution from the reaction, small-scale acidification was required in order to have a clear solution before injection into the HPLC column. After maximum conversion was reached, the reaction solution was finally acidified by 1% TFA in MeCN, pH 2-3. The crude reaction was also investigated via MALDI-TOF-MS (Sciex/Applied Biosystems 4800plus MaldiTOF/TOF analyser equipped with a Nd-YAG solid-state laser (355 nm, and a pulse frequency of 200 Hz) in order to confirm the product formation. The crude solution was immediately purified by either preparative or semi-preparative HPLC (see in peptide purification section). The purified peptide was collected and combined followed by lyophilisation in order to dry the target peptides.

MALDI-TOF-MS analysis. MALDI-TOF-MS evidence was acquired on a Sciex/Applied Biosystems 4800plus MaldiTOF/TOF analyser equipped with a Nd-YAG solid state laser (355 nm) and a pulse frequency of 200 Hz. For α-CHCA-matrix preparation (1 mL), 5 mg of α-cyano-4-hydroxycinnamic acid (α-CHCA) were dissolved in a solution containing acetonitrile (500 μL), milliQ water (480 μL), 1M ammonium citrate buffer (10 μL) and 10% TFA in miliQ water (10 μ). For the targeted peptides mass analysis, 0.5 μL of the α-CHCA matrix was first spotted on the MALDI plate with 0.5 μL of the sample spotted on top of it, and homogeneously mixed.

Liquid Chromatography-Electrospray ionization-Mass Spectrometry (LC-ESI-MS). LC-MS analyses were conducted on an Agilent 1100 Series HPLC instrument with diode array detector (DAD), equipped with a Phenomenex Kinetex® EVO/Phenomenex Kinetex C18® 100 Å (150 x 4.6 mm, 5 μm, at 35°C), hyphenated to an Agilent ESI-single quadrupole MS detector type VL. Mass detection operated in either positive mode or negative mode. A two-solvent system was used: 0.1% formic acid in miliQ water (A) and acetonitrile (B), using a gradient from 0% to 100% B for 15 minutes at a flow rate of 1.5 mL/min at 35 °C.

Peptide Purifications (preparative and semi-preparative HPLC). The purification of the linear peptides (40-50 µmol scale) was performed on an Agilent 218 preparative HPLC system with a UV-VIS dual-wavelength detector using a PrepPak® cartridge (Waters 1000, Delta-pak C18 100Å, system pressure 200-600 psi) using a two-solvent system A (0.1% TFA in miliQ water) and B (0.1% TFA in MeCN) with a flow rate of 65 mL/min at wavelength 214 nm. The gradient system for preparative HPLC was optimized from analytical HPLC (Chromolith® High resolution, RP-18e, 50-4.6 mm, 0-100% for 7 min at 35°C). The void volume (V_0) of preparative HPLC is around 5 min. In general, to generate a gradient profile, on the non-elution region, the increasing ratio of solvent B goes up 2% per minute whereas, in the elution region, solvent B goes up either 1% per minute or less than 1% per minute in order to have a good separation profile. Afterwards, sampling the fractions that potentially have expected peptide, followed by spotting on MALDI plate, and analysing each spot in order to confirm the presence of the desired peptide, took place. Finally, the fractions containing the targeted peptide were combined followed by a lyophilization process. The pure peptide was then subjected to LCMS in order to re-check its final purity (see supporting information in Supplementary Material for original chromatograms and MS spectra).

For semi-preparative HPLC (on a 5-10 µmol scale), the purification was conducted on an Agilent 218 solvent-delivery system with a UV-VIS dual wavelength detector using a Phenomenex column (AXIA packed Luna C18(2), 250 x 21.2 mm, 5 µm particle size, 35°C) with a flow rate of 17.5 mL/min. The stapled/linear peptides were eluted with a gradient using a two-solvent system: A (0.1% TFA in miliQ water) and B (MeCN). The method used had a linear gradient from 0 to 100% B in 26 minutes and followed up the elution at 214 and 254 nm. For a hydrophobic peptide, the gradient profile can change to a higher percentage of solvent B.

For semi-preparative HPLC (< 5 µmol scale), the purification was conducted on an Agilent 1200 series HPLC instrument with quaternary gradient pump equipped with a Luna C18 (250 x 10 mm, 5 µm particle size, 100Å, 35°C) with a flow rate of 4.0 mL/min, and diode-array detector (DAD) . The interesting peptides were eluted with a gradient using two mobile-phase system: A (0.1% TFA in miliQ water) and B (MeCN), and followed up the purification profile at 214 and 254 nm.

Enzyme stability: α-Chymotrypsin. A peptide stock solution was first prepared in DMSO at 1 mM concentration. To 21 µL of test peptide solution was added 609 µL of Tris buffer solution (pH 7.5), (i.e., 30 µM, dissolved in Tris buffer, pH 7.5), resulting in a final DMSO concentration of 10%. Next, 70 µL of α-chymotrypsin type II from bovine pancreas (2.5 µg/mL in Tris buffer, pH 7.5 -> final concentration 0.25 µg/mL, with pre-activation of the enzyme at 37°C for 5 min) was added and the mixture was incubated at 37 °C, 900 rpm. Afterwards, 40 µL of sample was taken into a separate HPLC vial followed by addition of a half volume of 0.2 % TFA in acetonitrile (20 µL, with the presence of 0.1 mM Fmoc-Val-OH as an internal standard) and further analyzed with RP-HPLC (Kinetex® column, flow rate =1.5 mL/min), gradient 0-100% acetonitrile in water + 0.1% TFA in 6 min). The digestion reaction was followed at different time points including 0, 30 min, 1h, 2h, 3h, 4h and 5 h.

Positive controls (without α-chymotrypsin)

Tris buffer solution (pH 7.5), 291 µL, was added to 9 µL of peptide solution (30 µM, dissolved in Tris buffer, pH 7.5, resulting in a final DMSO concentration of 10%), and the mixture was incubated at 37 °C, 900 rpm without α-chymotrypsin. Afterwards, 40 µL of the sample was taken into separate HPLC vial, and further analyzed with a Kinetex® C18 100 Å column (150 x 4.6 mm, 5 µm, at 35°C, flow rate 1.5 mL/min).

Negative controls (without peptides of interest)

Tris buffer solution (pH 7.5), 291 µL, was added to a DMSO solution (10% DMSO = 9 µL), and the mixture was incubated at 37 °C, 900 rpm. Afterwards, 40 µL of sample was taken into separate HPLC vial, and further analyzed with Kinetex C18 100 Å (150 x 4.6 mm, 5 µm, at 35°C, flow rate 1.5 mL/min).

Human serum stability. A peptide solution was first prepared in DMSO stock at 1 mM concentration. Human serum from male AB plasma (Sigma-Aldrich) was prepared by centrifugation at 17,000 g for 10 min at room temperature to remove the lipid components in order to obtain 100% serum. Serum with a pretreatment step was then diluted with 1X PBS, pH 7.4 into working concentrations (25, 12.5 and 6.25%, respectively) as stock solutions. The respective peptide stock solution (1 mM) was aliquoted, 20 μL (100 μM peptide) followed by addition into the various serum concentrations (180 μL). The mixture was allowed to shake at 37°C, 1000 rpm for 24 hours (final end point). The 20-μL samples were taken out, followed by the addition of ,80 μL of quenching solution (0.2% TFA in MeCN containing 0.018 mM Fmoc-Val-OH as internal standard). Afterwards, the sample was cooled down in an ice bath for protein precipitation (5 min) followed by centrifugation at 17,000 g for 10 min to remove the precipitated particles. Supernatant liquids (80 μL) were subsequently transferred into an HPLC vial for each time point. The solution was subjected to analysis with Kinetex® C18 100 Å (150 x 4.6 mm, 5 μm, at 35°C, flow rate 1.5 mL/min).
Positive controls
1X PBS buffer (pH 7.4) replaced the human serum followed by addition of the same concentration of peptide stock (1 mM).
Negative controls
1X PBS buffer (pH 7.4) replaced the human serum without peptide stock solution (1 mM).

Circular Dichroism (CD) Spectroscopy. CD spectra of the TATDOCK peptides were obtained using a JASCO J7100 instrument (Tokyo, Japan), equipped with a HAAKE cryostat temperature-controlled cell holder at 25°C. CD spectra are reported as the mean residue molar ellipticity, [θ], with units of degrees square centimeter per decimole (deg x cm^2/dmol), calculated by the equation (below):

$$[\theta] = (\theta_{obs} \times MRW)/(10lc)$$

where θ_{obs} is the ellipticity in millidegrees, MRW is the mean residue molecular weight (molecular weight of the peptide divided by the number of amino acid residues), l is the path length of the cuvette in centimeters, and c is the peptide concentration in milligrams per milliliter (mg/mL). The CD spectra were recorded at 50 nm/min scan rate, a bandwidth of 1 nm, a data pitch of 0.1 nm, a response of 2 sec, a wavelength range of 185–260 nm, and a 1-cm path length cell.
Each spectrum was an average of nine scans. Baselines were corrected by subtracting the solvent contribution. The CD spectra for all peptides of interest were measured at 20 μM in miliQ water and 50% of 2,2,2-Trifluoroethanol (TFE) for each TATDOCK peptide, respectively.

Peptide concentration determination. To prepare TATDOCK peptide stock solutions, the peptide powders were aliquoted into 2-mL Eppendorf tubes followed by dilution with miliQ water. Afterwards, the concentration was determined using the Thermo Scientific™ NanoDrop™ One droplet reader at λ 280 nm (triplicate per sample). The calculation of peptide concentration was obtained from the Beer-Lambert Equation (see below):

$$c = A_{280}/(\varepsilon \times b)$$

Where A280 is UV absorbance in absorbance units (AU), ε is wavelength-dependent molar-absorptivity coefficient (or extinction coefficient) in liter/mol^{-cm}, b is pathlength in cm, and c is analyte concentration in moles/liter or molarity (M).

Acknowledgements

Supplementary Material

LCMS and NMR spectra of the deoxycholic acid derivative, LC-ESI-MS and MALDI-TOF analysis of peptides and details of CD measurements are given in the supplementary material file associated with this manuscript.

References

1. de Las Rivas, J.; Fontanillo, C. *PLoS Comput Biol.* **2010**, *6*, 1–8.
   https://doi.org/10.1371/journal.pcbi.1000807
2. Meisel, J. W.; Hamilton, A. D. Supramolecular Approaches to Protein Recognition. In *Supramolecular Protein Chemistry: Assembly, Architecture and Application*; Crowley, P. B., Ed.; The Royal Society of Chemistry, 2020.
   https://doi.org/10.1039/9781788019798-00001
3. Bullock, B. N.; Jochim, A. L.; Arora, P. S. *J. Am. Chem. Soc.* **2011**, *133*, 14220–14223.
   https://doi.org/10.1021/ja206074j
4. Jochim, A. L.; Arora, P. S.. *Mol. Biosyst.* **2009**, *5*, 924–926.
   https://doi.org/10.1039/b903202a
5. Tian, Y.; Li, J.; Zhao, H.; Zeng, X.; Wang, D.; Liu, Q.; Niu, X.; Huang, X.; Xu, N.; Li, Z. *Chem. Sci.* **2016**, *7*, 3325–3330.
   https://doi.org/10.1039/c6sc00106h
6. Lau, Y. H.; De Andrade, P.; Wu, Y.; Spring, D. R. *Chem Soc Rev* **2015**, 91–102.
    https://doi.org/10.1039/c4cs00246f
7. Hill, T. A.; Shepherd, N. E.; Diness, F.; Fairlie, D. P. *Angew. Chem., Int. Ed. Engl.* **2014**, *53*, 13020–13041.
   https://doi.org/10.1002/anie.201401058
8. Bird, G. H.; Christian Crannell, W.; Walensky, L. D. *Curr. Protoc. Chem. Biol.* **2011**, *3*, 99–117.
   https://doi.org/https://doi.org/10.1002/9780470559277.ch110042
9. Moiola, M.; Memeo, M. G.; Quadrelli, P. *Molecules* **2019**, *24,* 3654.
   https://doi.org/10.3390/molecules24203654
10. Walensky, L. D.; Bird, G. H. *J. Med. Chem.* **2014**, 6275–6288.
    https://doi.org/10.1021/jm4011675
11. Komander, D.; Patel, M.; Laurin, M.; Fradet, N.; Pelletier, A.; Barford, D.; Côté, J.-F.; Adams, J. C. *Mol. Biol. Cell.* **2008**, *19*, 4837–4851.
    https://doi.org/10.1091/mbc.E08
12. Stevenson, C.; de la Rosa, G.; Anderson, C. S.; Murphy, P. S.; Capece, T.; Kim, M.; Elliott, M. R. *J. Immunol.* **2014**, *192*, 6062–6070.

https://doi.org/10.4049/jimmunol.130334

13. Sanui, T.; Inayoshi, A.; Noda, M.; Iwata, E.; Stein, J. V.; Sasazuki, T.; Fukui, Y. *Blood* **2003**, *102*, 2948–2950.
https://doi.org/10.1182/blood-2003-01-0173

14. Li, H.; Yang, L.; Fu, H.; Yan, J.; Wang, Y.; Guo, H.; Hao, X.; Xu, X.; Jin, T.; Zhang, N. *Nat. Commun.* **2013**, *4,* 1706.
https://doi.org/10.1038/ncomms2680

15. Wang, J.; Dai, J. M.; Che, Y. L.; Gao, Y. M.; Peng, H. J.; Liu, B.; Wang, H.; Linghu, H. *Int. J. Gynecol. Cancer* **2014**, *24*, 844–850.
https://doi.org/10.1097/IGC.0000000000000137

16. Capala, M. E.; Vellenga, E.; Schuringa, J. J. *PLoS One* **2014**, *9*, e111568
https://doi.org/10.1371/journal.pone.0111568

17. Hanawa-Suetsugu, K.; Kukimoto-Niino, M.; Mishima-Tsumagari, C.; Akasaka, R.; Ohsawa, N.; Sekine, S.; Ito, T.; Tochio, N.; Koshiba, S.; Kigawa, T.; Terada, T.; Shirouzu, M.; Nishikimi, A.; Uruno, T.; Katakai, T.; Kinashi, T.; Kohda, D.; Fukui, Y.; Yokoyama, S. *PNAS* **2012**, *109*, 3305–3310.
https://doi.org/10.1073/pnas.1113512109 .

18. Arandjelovic, S.; Perry, J. S. A.; Lucas, C. D.; Penberthy, K. K.; Kim, T. H.; Zhou, M.; Rosen, D. A.; Chuang, T. Y.; Bettina, A. M.; Shankman, L. S.; Cohen, A. H.; Gaultier, A.; Conrads, T. P.; Kim, M.; Elliott, M. R.; Ravichandran, K. S. *Nat. Immunol.* **2019**, *20*, 141–151.
https://doi.org/10.1038/s41590-018-0293-x

19. Arandjelovic, S.; Perry, J. S. A.; Zhou, M.; Ceroi, A.; Smirnov, I.; Walk, S. F.; Shankman, L. S.; Cambré, I.; Onengut-Gumuscu, S.; Elewaut, D.; Conrads, T. P.; Ravichandran, K. S. *Nat. Commun.* **2021**, *12*, 4974.
https://doi.org/10.1038/s41467-021-25239-6

20. Muppidi, A.; Doi, K.; Edwardraja, S.; Drake, E. J.; Gulick, A. M.; Wang, H. G.; Lin, Q. *J. Am. Chem. Soc.* **2012**, *134*, 14734–14737.
https://doi.org/10.1021/ja306864v

21. Muppidi, A.; Zhang, H.; Curreli, F.; Li, N.; Debnath, A. K.; Lin, Q. *Bioorg. Med. Chem. Lett.* **2014**, *24*, 1748–1751.
https://doi.org/10.1016/j.bmcl.2014.02.038

22. Muppidi, A.; Doi, K.; Ramil, C. P.; Wang, H. G.; Lin, Q. *Tetrahedron* **2014**, *70*, 7740–7745.
https://doi.org/10.1016/j.tet.2014.05.104

23. Fairlie, D. P.; Dantas de Araujo, A. Review Stapling Peptides Using Cysteine Crosslinking. *Biopolymers*. John Wiley and Sons Inc. **2016**, pp 843–852.
https://doi.org/10.1002/bip.22877

24. Tian, Y.; Zou, H.; An, P.; Zhou, Z.; Shen, W.; Lin, Q. *Tetrahedron* **2019**, *75*, 286–295.
https://doi.org/10.1016/j.tet.2018.11.060

25. Leduc, A.-M.; Trent, J. O.; Wittliff, J. L.; Bramlett, K. S.; Briggs, S. L.; Chirgadze, N. Y.; Wang, Y.; Burris, T. P.; Spatola, A. F. *PNAS* **2003**, *100*, 11273-11278
https://doi.org/10.1073/pnas.1934759100

26. Barthe, P.; Rochette, S.; Vita, C.; Roumestand, C. *Protein Sci.* **2000**, *9*, 942-955.
https://doi.org/10.1110/ps.9.5.942

27. Kumita, J. R.; Smart, O. S.; Woolley, G. A. *PNAS* **2000**, *97*, 3803–3808.
https://doi.org/10.1073/pnas.97.8.3803

28. Bechara, C.; Sagan, S. *FEBS Letters*. **2013**, 1693–1702.

https://doi.org/10.1016/j.febslet.2013.04.031

29. Koren, E.; Apte, A.; Sawant, R. R.; Grunwald, J.; Torchilin, V. P. *Drug. Deliv.* **2011**, *18*, 377–384.
https://doi.org/10.3109/10717544.2011.567310

30. Patel, S. G.; Sayers, E. J.; He, L.; Narayan, R.; Williams, T. L.; Mills, E. M.; Allemann, R. K.; Luk, L. Y. P.; Jones, A. T.; Tsai, Y. H. *Sci. Rep.* **2019**, *9*, 6298.
https://doi.org/10.1038/s41598-019-42456-8

31. Subirós-Funosas, R.; Prohens, R.; Barbas, R.; El-Faham, A.; Albericio, F. *Chem. – Eur. J.* **2009**, *15*, 9394–9403.
https://doi.org/10.1002/chem.200900614

32. Chen, X. T.; Wang, J. Y.; Ma, Y. N.; Dong, L. Y.; Jia, S. X.; Yin, H.; Fu, X. Y.; Du, S. S.; Qi, Y. K.; Wang, K. W. *J. Pept. Sci.* **2022**, *28*, e3368
https://doi.org/10.1002/psc.3368

33. Carpino, L. A.; Ionescu, D.; El-Faham, A. *J. Org. Chem*. **1996**, *61*, 2460-2465.
https://doi.org/10.1021/jo950912x

34. Caporale, A.; Doti, N.; Monti, A.; Sandomenico, A.; Ruvo, M. *Peptides* **2018**, *102*, 38–46.
https://doi.org/10.1016/j.peptides.2018.02.006

35. D'Ercole, A.; Pacini, L.; Sabatino, G.; Zini, M.; Nuti, F.; Ribecai, A.; Paio, A.; Rovero, P.; Papini, A. M. *Org. Process Res. Dev.* **2021**, 2754–2771.
https://doi.org/10.1021/acs.oprd.1c00368

36. Jad, Y. E.; Khattab, S. N.; de la Torre, B. G.; Govender, T.; Kruger, H. G.; El-Faham, A.; Albericio, F. *Eur. J. Org. Chem.* **2015**, *14*, 3116–3120.
https://doi.org/10.1002/ejoc.201500142

37. El-Faham, A.; Albericio, F. *Chem. Rev.* **2011**, 6557–6602.
https://doi.org/10.1021/cr100048w

38. Jo, H.; Meinhardt, N.; Wu, Y.; Kulkarni, S.; Hu, X.; Low, K. E.; Davies, P. L.; Degrado, W. F.; Greenbaum, D. C. *J. Am. Chem. Soc.* **2012**, *134*, 17704–17713.
https://doi.org/10.1021/ja307599z

39. Meng, G.; Pu, J.; Li, Y.; Han, A.; Tian, Y.; Xu, W.; Zhang, T.; Li, X.; Lu, L.; Wang, C.; Jiang, S.; Liu, K. *J. Med. Chem.* **2019**, *62*, 8773–8783.
https://doi.org/10.1021/acs.jmedchem.9b00882

40. Ruiz García, Y.; Iyer, A.; Van Lysebetten, D.; Vladimir Pabon, Y.; Louage, B.; Honcharenko, M.; De Geest, B. G.; Edvard Smith, C. I.; Strömberg, R.; Madder, A. *Chem. Comm.* **2015**, *51*, 17552–17555 .
https://doi.org/10.1039/c5cc07097j

41. Kemp, D. S.; Allen, T. J.; Oslick, S. L.; Boyd, J. G. *J. Am. Chem. Soc.* **1996**, *118*, 4240–4248.
https://doi.org/10.1021/ja9529100

42. Culik, R. M.; Abaskharon, R. M.; Pazos, I. M.; Gai, F. *J. Phys. Chem. B* **2014**, *118*, 11455–11461.
https://doi.org/10.1021/jp508056w

43. Shepherd, N. E.; Hoang, H. N.; Abbenante, G.; Fairlie, D. P. *J. Am. Chem. Soc.* **2005**, *127*, 2974–2983.
https://doi.org/10.1021/ja0456003

44. Grigoryan, G.; Reinke, A. W.; Keating, A. E. *Nature* **2009**, *458*, 859–864.
https://doi.org/10.1038/nature07885

45. Crooks, R. O.; Rao, T.; Mason, J. M. *J. Biol. Chem.* **2011**, *286*, 29470–29479.
https://doi.org/10.1074/jbc.M111.221267

46. Banerjee, R.; Sheet, T. *Proteins* **2017**, *85*, 1975–1982.

https://doi.org/10.1002/prot.25351

47. Coughlin, S. R. *Nature* **2000**, *407*, 258–264.
https://doi.org/10.1038/35025229

48. Appel, W. *Clin. Biochem.* **1986**, *19*, 317–322.
https://doi.org/https://doi.org/10.1016/S0009-9120(86)80002-9

49. Hedstrom, L. *Chem. Rev.* **2002**, *102*, 4501–4523.
https://doi.org/10.1021/cr000033x

50. Kumar, A.; Venkatesu, P. *Chem. Rev.* **2012**, 4283–4307.
https://doi.org/10.1021/cr2003773

51. Greenfield, N. J. *Nat. Protoc.* **2006**, *1*, 2527–2535.
https://doi.org/10.1038/nprot.2006.204